Article

Dissipation of Electronic Excitation Energy within a C [6:0]-Hexaadduct Carrying 12 Pyropheophorbide *a* Moieties

Matthias Helmreich, Eugeny A. Ermilov, Matthias Meyer, Norbert Jux, Andreas Hirsch, and Beate Rder

J. Am. Chem. Soc., **2005**, 127 (23), 8376-8385• DOI: 10.1021/ja0503581 • Publication Date (Web): 20 May 2005

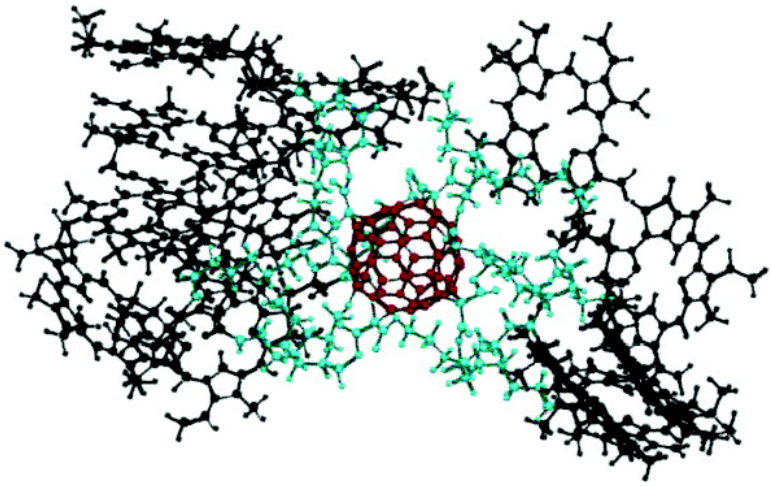

J|A|C|S
ARTICLES
Published on Web 05/20/2005

Dissipation of Electronic Excitation Energy within a C_{60} [6:0]-Hexaadduct Carrying 12 Pyropheophorbide *a* Moieties

Matthias Helmreich,[†] Eugeny A. Ermilov,[‡] Matthias Meyer,[‡] Norbert Jux,*[,†] Andreas Hirsch,*[,†] and Beate Röder*[,‡]

Contribution from the Institut für Organische Chemie, Universität Erlangen-Nürnberg, Henkestrasse 42, D-91054 Erlangen, Germany, and Institut für Physik, Photobiophysik, Humboldt-Universität zu Berlin, Newtonstrasse 15, D-12489 Berlin, Germany

Received February 11, 2005; E-mail: roeder@physik.hu-berlin.de

Abstract: The synthesis and photophysical studies of a fullerene [6:0]-hexaadduct that carries 12 pyropheophorbide *a* units are reported. The synthesis started with the malonate **1**, which was coupled under template conditions to C_{60} to give the hexaadduct **2**. After removal of the protecting group with acid the dodecakis amino-substituted precursor compound **3** was generated. **3** was not isolated but directly reacted with the *N*-succinimid ester **4** of pyropheophorbide *a* (**5**), which delivered the desired fullerene [6:0]-hexaadduct **6** in excellent yield. The photophysical properties of **6** were studied and compared with those of the fullerene [5:1]-hexaadduct **7** with six pyropheophorbide *a* groups and the bispyropheophorbide *a*-fullerene [5:1]-hexaadduct **8**. The pyropheophorbide *a* units in **6** undergo after light absorption very efficient energy transfer as well as partly excitonic interaction. The last process results in formation of energy traps, which could be resolved experimentally. Compared to the reference compounds **7** and **8**, **6** has a higher probability of trap formation due to a higher local concentration of dye molecules and shorter distances between them. As a consequence, the excitation energy is delivered rapidly (within 23 ps) to the traps, resulting in decreases of the fluorescence, intersystem crossing, and singlet oxygen quantum yields in comparison with the values of the reference compounds.

Introduction

The unique photophysical and photochemical properties of fullerenes have led to the synthesis of a large number of compounds in which fullerenes are covalently linked to different kinds of photoactive groups, in particular porphyrins. Some of these complexes could serve as artificial light harvesting systems due to the high capability of the fullerene moiety to act as an electron acceptor or even an electron accumulator.[1−8] Furthermore, these contributions are important steps toward the understanding and simulating of the photosynthetic apparatuses and their guiding principles. It comes with no surprise that chlorins were utilized extensively in electron-transfer studies because such compounds can be regarded as model compounds for the photosynthetic reaction center with naturally occurring electron donors.[9−19]

C_{60} can be used as a versatile building block for the construction of globular dendrimers,[20−27] which opens up ways for biomedical applications of fullerene-based molecular systems. One possibility is the use of the fullerene as functional core of an efficient multiplier in modular drug delivery systems

[†] Universität Erlangen-Nürnberg.
[‡] Humboldt-Universität zu Berlin.

(1) Imahori, H.; Sakata, Y. *Adv. Mater.* **1997**, *9*, 537−546.
(2) Kuciauskas, D.; Liddell, P. A.; Lin, S.; Johnson, T. E.; Weghorn, S. J.; Lindsey, J. S.; Moore, A. L.; Moore, T. A.; Gust, D. *J. Am. Chem. Soc.* **1999**, *121*, 8604−8614.
(3) Rio, Y.; Nierengarten, J.-F. *Tetrahedron Lett.* **2002**, *43*, 4321−4324.
(4) Imahori, H.; Mori, Z.; Matano, Y. *J. Photochem. Photobiol., C* **2003**, *4*, 51−83.
(5) Imahori, H.; Fukuzumi, S. *Adv. Funct. Mater.* **2004**, *14*, 525−536.
(6) Fukuzumi, S.; Hasobe, T.; Ohkubo, K.; Crossley, M. J.; Kamat, P. V.; Imahori, H. *J. Porphyrins Phthalocyanines* **2004**, *8*, 191−200.
(7) Guldi, D. M.; Fukuzumi, S. *J. Porphyrins Phthalocyanines* **2002**, *6*, 289−295.
(8) Bonifazi, D.; Scholl, M.; Song, F.; Echegoyen, L.; Accorsi, G.; Armaroli, N.; Diederich, F. *Angew. Chem., Int. Ed.* **2003**, *42*, 4966−4970.
(9) Ohkubo, K.; Kotani, H.; Shao, J.; Ou, Z.; Kadish, K. M.; Li, G.; Pandey, R. K.; Fujitsuka, M.; Ito, O.; Imahori, H.; Fukuzumi, S. *Angew. Chem., Int. Ed.* **2004**, *43*, 853−856.
(10) Helaja, J.; Tauber, A. Y.; Abel, Y.; Tkachenko, N. V.; Lemmetyinen, H.; Kilpelainen, I.; Hynninen, P. H. *J. Chem. Soc., Perkin Trans. 1* **1999**, 2403−2408.
(11) Tkachenko, N. V.; Rantala, L.; Tauber, A. Y.; Helaja, J.; Hynninen, P. H.; Lemmetyinen, H. *J. Am. Chem. Soc.* **1990**, *12*, 9378−9387.
(12) Efimov, A.; Tkatchenko, N. V.; Vainiotalo, P.; Lemmetyinen, H. *J. Porphyrins Phthalocyanines* **2001**, *5*, 835−838.
(13) Vlassiouk, I.; Smirnov, S.; Kutzki, O.; Wedel, M.; Montforts, F. P. *J. Phys. Chem. A* **2002**, *106*, 8657−8666.
(14) Zheng, G.; Dougherty, T. J.; Pandey, R. K. *Chem. Commun.* **1999**, 2469−2470.
(15) Ohkubo, K.; Imahori, H.; Shao, J.; Ou, Z.; Kadish, K. M.; Chen, Y.; Zheng, G.; Pandey, R. K.; Fujitsuka, M.; Ito, O.; Fukuzumi, S. *J. Phys. Chem. A* **2002**, *106*, 10991−10998.
(16) Fukuzumi, S.; Ohkubo, K.; Imahori, H.; Shao, J.; Ou, Z.; Zheng, G.; Chen, Y.; Pandey, R. K.; Fujitsuka, M.; Ito O.; Kadish, K. *J. Am. Chem. Soc.* **2001**, *123*, 10676−10683.
(17) Holzwarth, A. R.; Batterle, M.; Muller, M. G.; Ma, Y. Z.; Prokhorenko, V. *Pure Appl. Chem.* **2001**, *73*, 469−474.
(18) Kutzki, O.; Walter, A.; Montforts, F. P. *Helv. Chim Acta* **2000**, *83*, 2231−2245.
(19) Montforts, F. P.; Kutzki, O. *Angew. Chem., Int. Ed.* **2000**, *39*, 599−601.
(20) Nierengarten, J.-F. *New J. Chem.* **2004**, *28*, 1177−1191.
(21) Camps, X.; Schönberger, H.; Hirsch, A. *Chem.−Eur. J.* **1997**, *3*, 561−567.

 10.1021/ja0503581 CCC: $30.25

Scheme 1. Chemical Structure of C_{60}-Bispyropheophorbide *a* with (**8**) and without (**9**) Additional Diethyl Malonate Addends in the Octahedral Positions of the Fullerene

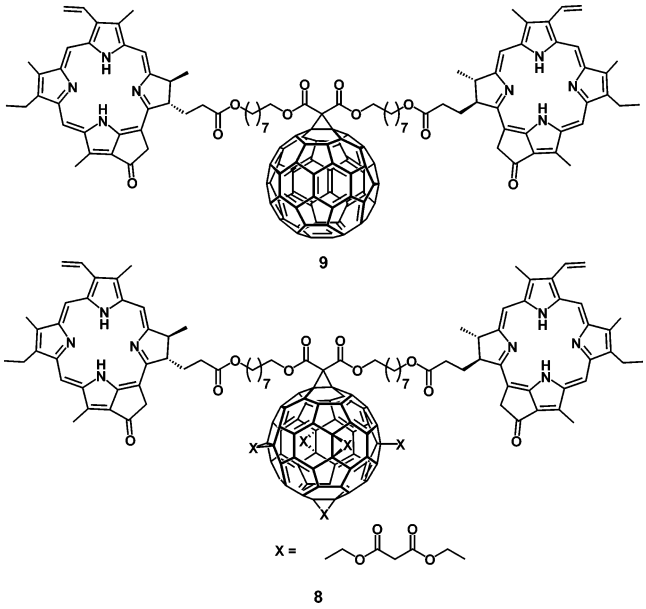

for the photodynamic therapy of tumors.[28,29] Consequently, the photosensitizers could be attached to $\mathbf{C_{60}}$ directly or via dendritic structures.[29]

Recently, we reported on the synthesis and photophysical properties of the novel fullerene supramolecules **8** and **9**, which carry two 13^2-demethoxycarbonylpheophorbide *a* (short: pyropheophorbide *a* or just pyroPheo) units each.[30−33] In the $\mathbf{C_{60}}$-bispyropheophorbide *a* conjugate **9** (see Scheme 1) the fullerene moiety strongly affects the photoactivity of the photosensitizer **5** due to the high electron-accepting capabilities mentioned above. As a result, a strong reduction of the fluorescence as well as of the singlet oxygen generation quantum yields was observed for **9** compared to those values of a nonfullerene reference compound.[31,34,35] If the conjugation of the π-system of the fullerene is broken up by the addition of five diethyl malonate addends in the remaining octahedral positions (as in **7** and **8**), the electron-accepting ability of the $\mathbf{C_{60}}$ moiety is strongly reduced and it acts only as a neutral attachment.[31]

Our next step was to expand the motif given in **8** to a larger system utilizing dendrimers as multiplying units: the hexapyropheophorbide *a*-$\mathbf{C_{60}}$ hexaadduct **7** has been synthesized.[33] Scheme 2 shows the chemical structure of **7**. In **7** the fluorescence as well as the singlet oxygen quantum yields were quenched compared to the values of **8**. The results were explained by applying a model of energy traps formed by two closely located excitonically interacting pyropheophorbide *a* molecules attached to the same fullerene moiety and efficient delivery of excitation to them via dipole−dipole Förster energy transfer.

In this article, we wish to report on the synthesis and comparative studies of the photophysical properties of a novel molecular system **6** containing 12 pyropheophorbide *a* moieties covalently linked to $\mathbf{C_{60}}$.

Experimental Section

Chemicals and Characterization of the Samples. $\mathbf{C_{60}}$ was obtained from Hoechst AG/Aventis and was separated from higher fullerenes by a plug filtration process.[36,37] Pyropheophorbide *a* was prepared according to literature procedures[38] from spinach or algae (*Chlorella* or *Urtica dioica*), and its purity was checked for each batch by ^{1}H NMR. Chemicals and solvents were used as received unless otherwise noted. Solvents were dried using standard procedures.[39] Column chromatography was performed on silica gel 32−63, 60 Å, MP Biomedicals. ^{1}H and ^{13}C NMR spectra were recorded on JEOL JMM EX 400 and JEOL GX 400 instruments. An asterisk indicates a resonance of a pyropheophorbide *a* proton or carbon atom; the atom indices are given according to the literature.[40] FAB mass spectrometry was performed with Micromass Zabspec and Varian MAT 311A machines. MALDI-TOF mass spectrometry was done on an AUTOFLEX machine from Bruker Daltonics GmbH. Standard UV/vis spectra were recorded on a Shimadzu UV-3102 PC UV/vis NIR scanning spectrophotometer. IR spectra were taken with either a Bruker Vector 22 spectrometer or an ASI React IR-1000 spectrometer. HPLC was performed with a Shimadzu liquid chromatograph LC-10AT equipped with an SCL-10AVP system controller, LC-8A preparative liquid chromatographs, a diode array detector, and a UV/vis detector, on a Nucleosil 100−5 column. All compounds decomposed prior to melting.

2. $\mathbf{C_{60}}$ (0.9 g, 1.25 mmol) was dissolved in 800 mL of dry toluene. 9,10-Dimethylanthracene (DMA) (2.6 g, 12.5 mmol) was added to that solution and stirred for 12 h at ambient temperature, after which **1** (6.3 g, 12.5 mmol) and CBr_4 (4.15 g, 12.5 mmol) were added. 1,8-Diazabicyclo[5.4.0]undec-7-ene (DBU) (2.24 mL, 15 mmol) dissolved in 20 mL of dry toluene was added dropwise, and the solution was stirred for 3 days at room temperature. The solvent was removed in vacuo, and the residue was chromatographed on silica gel with ethyl acetate/CH_2Cl_2 4:6 as eluent. The obtained fractions containing a mixture of pentakis- and hexakisadducts were further purified by

(22) (a) Dietel, E.; Hirsch A.; Eichhorn, E.; Hackbarth, S.; Röder, B. *J. Chem. Soc., Chem. Commun.* **1998**, 1981−1982. (b) Guldi, D. M.; Luo, C.; da Ros, T.; Prato, M.; Dietel, E.; Hirsch, A. *J. Chem. Soc., Chem. Commun.* **2000**, 375−376. (c) Guldi, D. M.; Luo, C.; Prato, M.; Dietel, E.; Hirsch, A. *J. Chem. Soc., Chem. Commun.* **2000**, 373−374. (d) Guldi, D. M.; Luo, C.; Prato, M.; Scheloske, M.; Dietel, E.; Bauer, W.; Hirsch, A. *J. Am. Chem. Soc.* **2001**, *123*, 9166−9167. (e) Sutton, L. R.; Scheloske, M.; Pirner, K. S.; Hirsch, A.; Guldi, D. M.; Gisselbrecht J.-P. *J. Am. Chem. Soc.* **2004**, *126*, 10370−10381.

(23) Hirsch, A.; Vostrowsky, O. *Top. Curr. Chem.* **2001**, *217*, 51−93.

(24) Hirsch, A.; Vostrowsky, O. *Eur. J. Org. Chem.* **2001**, 829−848.

(25) Brettreich, M.; Burghardt, S.; Böttcher, C.; Bayerl, T.; Bayerl, S.; Hirsch, A. *Angew. Chem., Int. Ed.* **2000**, *39*, 1845−1848.

(26) Herzog, A.; Hirsch, A.; Vostrowsky, O. *Eur. J. Org. Chem.* **2000**, 171−180.

(27) Nierengarten, J.-F.; Eckert, J.-F.; Rio, Y.; Carreon, M. D. P.; Gallani, J.-L.; Guillon, D. *J. Am. Chem. Soc.* **2001**, *123*, 9743−9748.

(28) Röder, B. In *Encyclopedia Analytical Chemistry*; Meyers, R. A., Ed.; Wiley: Chichester, 2000; pp 302−322.

(29) Camps, X.; Dietel, E.; Hirsch, A.; Pyo, S.; Echegoyen, L.; Hackbarth, S.; Röder, B. *Chem.−Eur. J.* **1999**, *5*, 2362−2373.

(30) Helmreich, M.; Hirsch, A.; Jux, N. *J. Porphyrins Phthalocyanines*, in press, 2005.

(31) Ermilov, E. A.; Al-Omari, S.; Helmreich, M.; Jux, N.; Hirsch, A.; Röder, B. *Chem. Phys.* **2004**, *301*, 27−31.

(32) In previous publications, acronyms for **6**−**9** were used: FHP12 for **6**, FHP6 for **7**, FHP1 for **8**, FP1 for **9**, respectively, in refs 30−35.

(33) Ermilov, E. A.; Hackbarth, S.; Helmreich, M.; Jux, N.; Hirsch, A.; Röder, B. *Opt. Commun.*, in press, 2005.

(34) Ermilov, E. A.; Al-Omari, S.; Helmreich, M.; Jux, N.; Hirsch, A.; Röder, B. *Opt. Commun.* **2004**, *234*, 245−252.

(35) Al-Omari, S.; Ermilov, E. A.; Helmreich, M.; Jux, N.; Hirsch, A.; Röder, B. *Appl. Phys. B* **2004**, *79*, 617−622.

(36) Reuther, U. Ph.D. Dissertation, University of Erlangen-Nürnberg, Erlangen, Germany, 2001.

(37) Isaacs, L.; Wehrsig, A.; Diederich F. *Helv. Chim. Acta* **1993**, *76*, 1231−1250.

(38) (a) Risch, N.; Reich, H.; Schormann, A.; Brockmann, H. *Liebigs Ann. Chem.* **1981**, 1519−1522. (b) Wasielewski, M. R.; Svec, W. A. *J. Org. Chem.* **1980**, *45*, 1969−1974.

(39) Perrin, D. D.; Amarego, W. L. F. *Purification of Laboratory Chemicals*, 3rd ed.; Pergamon Press: Oxford, 1988.

(40) (a) Closs, G. L.; Katz, J. J.; Pennington, F. C.; Thomas, M. R.; Strain, H. H. *J. Am. Chem. Soc.* **1963**, *85*, 3809−3821. (b) Smith, K. M.; Unsworth, J. F. *Tetrahedron* **1975**, *31*, 367−375.

Scheme 2. Chemical Structure of the Hexapyropheophorbide *a*-C_{60} Hexaadduct **7**

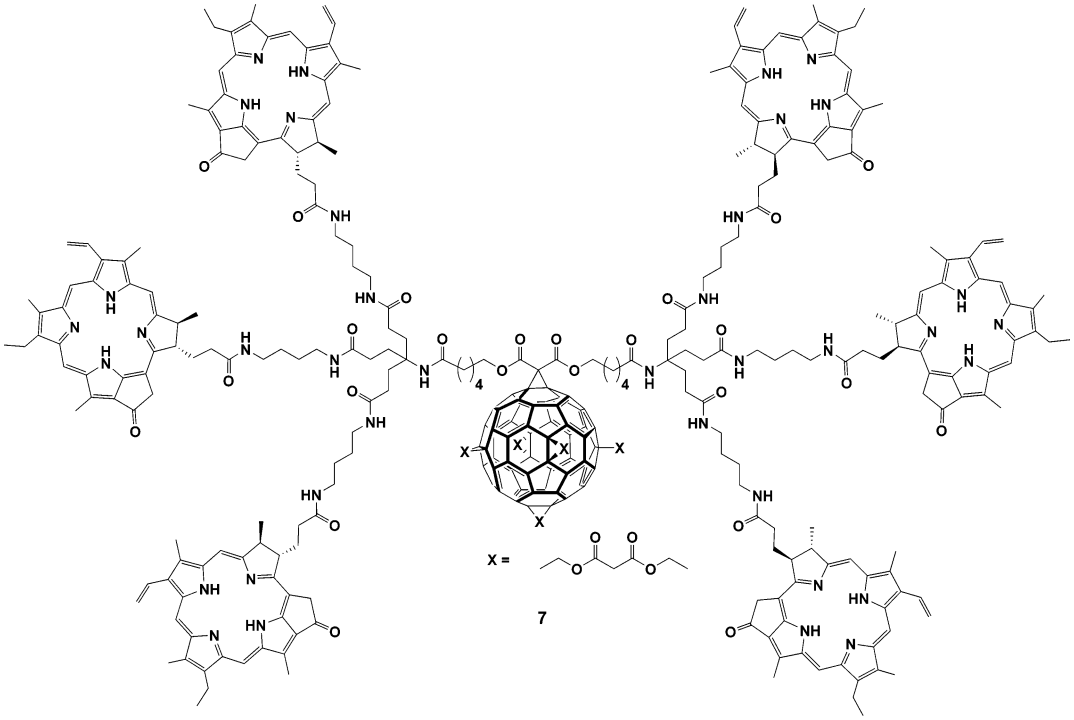

HPLC with ethyl acetate/CH_2Cl_2 1:3 as eluent. Yield 1.95 g (42%) based on $\mathbf{C_{60}}$. ^{1}H NMR (400 MHz, $CDCl_3$, 25 °C): δ 4.76 (bs, NH), 4.22 (t, 24H, ^3J = 6.5 Hz, OCH_2), 3.06 (q, 24H, ^3J = 6.3 Hz, NCH_2), 1.64 (m, 24H, OCH_2CH_2), 1.45 (m, 24H, CH_2), 1.40* (s, 108H, *t*-Bu), 1.31 (m, 48H, CH_2). ^{13}C NMR (100.5 MHz, $CDCl_3$, 25 °C): δ 163.8, 156.0, 145.7 ($\mathbf{C_{60}}$), 141.1 ($\mathbf{C_{60}}$), 78.9, 69.1 ($\mathbf{C_{60}}$), 66.9, 45.4, 40.5, 29.9, 28.4, 28.3, 26.4, 25.6. MS (FAB, NBA): *m*/*z* 3724 (M^+), 3667 (M^+-*t*-Bu), 3624 (M^+-BOC), 3568 (M^+-2x-*t*-Bu), 3525 (M^+-2x-BOC), 3424 (M^+-3x-BOC), 3324 (M^+-4x-BOC), 3224 (M^+-5x-BOC), 3124 (M^+-6x-BOC). UV/vis (CH_2Cl_2): λ_{max} (ϵ, M^{-1} cm^{-1}) 243 (97 700), 281 (77 000), 439 (1500). IR (KBr): ν 3414, 2932, 2858, 1746, 1714, 1521, 1365, 1265, 1169, 715. $C_{210}H_{264}N_{12}O_{48}$ (3724.39), calcd: C, 67.72; H, 7.14; N, 4.51, found: C, 67.15; H, 7.25; N, 4.52.

4. Pyropheophorbide *a* (**5**) (536 mg, 1.0 mmol), *N*-hydroxysuccinimid (NHS) (140 mg, 1.2 mmol), and DMAP (24 mg, 0.2 mmol) were dissolved in 50 mL of dry CH_2Cl_2 in a N_2 atmosphere. The solution was cooled to 0 °C. *N*-(3-Dimethylaminopropyl)-*N*-ethylcarbodiimid (EDC) (270 mg, 1.4 mmol) was added, and the mixture was stirred for 16 h at room temperature. The solvent was removed in vacuo, and the residue was chromatographed on silica gel with CH_2Cl_2/acetone 9:1 as eluent. Yield 253 mg (41%) based on pyropheophorbide *a*. ^{1}H NMR (400 MHz, $CDCl_3$, 25 °C): δ 9.25* (s, 1H, β-H), 9.15* (s, 1H, α-H), 8.50* (s, 1H, δ-H), 7.84* (dd, 1H, ^3J = 11.5 Hz, 17.8 Hz, 2a), 6.18* (dd, 1H, ^2J = 1.5 Hz, ^3J = 17.8 Hz, 2b), 6.08* (dd, 1H, ^2J = 1.5 Hz, ^3J = 11.5 Hz, 2b), 5.17* (d, 1H, ^2J = 19.9 Hz, 10), 5.09* (d, 1H, ^2J = 19.9 Hz, 10), 4.45* (dq, 1H, ^3J = 7.3 Hz, ^3J = 2.0 Hz, 8), 4.35* (dt, 1H, ^3J = 9.8 Hz, ^3J = 2.0 Hz, 7), 3.55* (s, 3H, 5a), 3.49* (q, 2H, ^3J = 8.5 Hz, 4a), 3.34* (s, 3H, 1a), 3.06* (s, 3H, 1a), 2.80* (m, 2H, 7a/b), 2.80 (bs, 4H, NHS−CH_2), 2.60* (m, 1H, 7a/7b), 2.20* (m, 1H, 7a/7b), 1.79* (d, 3H, ^3J = 7.3 Hz, 8a), 1.60* (t, 3H, ^3J = 7.7 Hz, 4b), 0.23* (bs, 1H, NH), −1.90* (s, 1H, NH). ^{13}C NMR (100.5 MHz, $CDCl_3$, 25 °C): δ 196.1, 170.9, 169.0, 168.2, 159.5, 154.9, 150.5, 148.8, 144.7, 141.4, 137.6, 135.9, 135.8, 135.6, 131.4, 130.4, 130.0, 128.1, 122.3, 105.9, 103.8, 97.0, 92.9, 76.7, 50.29, 49.7, 47.8, 29.5, 28.1, 25.5, 23.0, 19.2, 17.3, 12.0, 11.9, 11.0. MS (FAB, NBA): *m*/*z* 632 (M^+). UV/vis (CH_2Cl_2): λ_{max} (ϵ, M^{-1} cm^{-1}) 322 (20 600), 413 (108 300), 476 (4000), 508 (10 600), 538 (9500), 609 (8000), 666 (46 000). IR (ATR): ν 2966, 2929, 2861, 1808, 1785, 1739, 1617, 1499, 1349, 1210, 1061, 980, 820. $C_{37}H_{37}N_5O_5$*CH_2Cl_2 (716.65), calcd: C, 63.69; H, 5.49; N, 9.77, found: C, 63.35; H, 5.89; N, 10.31.

6. 2 (55 mg, 0.015 mmol) was dissolved in 40 mL of a methanolic HCl solution (~1.25 M) and was stirred for 24 h at room temperature. The solvent was removed, and the orange residue dissolved in 50 mL of brine. CH_2Cl_2 (50 mL) and triethylamine (100 μL) were added, and the organic layer was washed twice with brine. After being dried over Na_2SO_4, **4** (170 mg, 0.27 mmol) was added, and the solution was stirred for 72 h at room temperature. The solvent was removed in vacuo, and the residue was purified by size exclusion chromatography (1. Bio-beads SX3; 2. Bio-beads SX1, $CHCl_3$). Yield 97 mg (74%) based on **2**. ^{1}H NMR (400 MHz, $CDCl_3$, 25 °C): δ 8.81* (bs, 12H, β-H), 8.49* (bs, 12H, α-H), 8.29* (bs, 12H, δ-H), 7.46* (dd, 12H, ^3J = 11.6 Hz, 17.8 Hz, 2a), 6.17 (bs, 12H, NH), 5.88* (d, 12H, ^3J = 17.8 Hz, 2b), 5.81* (d, 12H, ^3J = 11.6 Hz, 2b), 4.90* (d, 12H, ^2J = 19.4 Hz, 10), 4.65* (d, 12H, ^2J = 19.4 Hz, 10), 4.21* (bs, 12H, 7), 3.94* (bs, 12H, 8), 3.94 (bs, 24H, O−CH_2), 3.13* (bs, 24H, 4a), 2.99* (s, 36H, 5a), 2.91* (bs, 36H, 1a), 2.78 (bs, 24H, N−CH_2), 2.68* (bs, 36H, 3a), 2.38* (m, 12H, 7a/b), 2.06* (m, 24H, 7a/b), 1.85* (m, 12H, 7a/b), 1.53* (d, 36H, ^3J = 6.9 Hz, 8a), 1.32* (t, 36H, ^3J = 7.3 Hz, 4b), 1.32 (bs, 24H, CH_2), 0.98 (bs, 72H, CH_2), −0.22* (bs, 12H, NH), −2.21* (s, 12H, NH). ^{13}C NMR (100.5 MHz, $CDCl_3$, 25 °C): δ 195.8, 172.3, 171.5, 166.9, 163.6, 160.4, 154.5, 150.0, 148.4, 145.6, 144.4, 141.0, 137.0, 135.6, 135.4, 131.1, 131.1, 129.5, 128.7, 127.3, 122.0, 105.6, 103.2, 96.5, 92.7, 69.0, 66.7, 51.6, 49.6, 47.8, 45.5, 39.1, 32.8, 31.4, 30.2, 29.0, 28.0, 26.2, 25.3, 22.7, 18.9, 17.1, 11.8, 11.2, 10.8. MS (MALDI-TOF, 2,5-dihydroxybenzoic acid): *m*/*z* 8724.3 (calcd 8722.6). UV/vis (CH_2Cl_2): λ_{max} (ϵ, M^{-1} cm^{-1}) 279 (251 000), 323 (309 000), 400 (868 000), 413 (858 000), 510 (99 200), 540 (83 700), 613 (78 900), 669 (395 000). IR (ATR): ν 2962, 2925, 2861, 1742, 1683, 1617, 1497, 1260, 1218, 1057, 978, 795, 671. $C_{546}H_{552}N_{60}O_{48}$*4$CHCl_3$ (9200.11), calcd: C, 71.80; H, 6.09; N, 9.13, found: C, 71.85; H, 5.93; N, 9.21.

Absorption and Steady-State Fluorescence. For the photophysical investigations, all samples were dissolved in DMF (Aldrich) of spectroscopic grade. The ground-state absorption spectra were recorded at room temperature using a commercial spectrophotometer Shimadzu UV-2501PC. Steady-state fluorescence spectra were measured in 1 cm × 1 cm quartz optical cells using a combination of a cw-Xenon lamp

(XBO 150) and a monochromator (Lot-Oriel, bandwidth 10 nm) for excitation and a polychromator with a cooled CCD matrix as a detector system (Lot-Oriel, Instaspec IV).[41] The optical density (OD) of all samples during the fluorescence measurements was 0.2 at the maximum of absorption Q-band corresponding to concentrations of 10^{-6} to 10^{-7} M.

Fluorescence Decay. Fluorescence decay times were measured by a time-correlated single photon counting (TCSPC) setup containing an SPC 630 plug-in card (Becker Hickel, Berlin) and a multichannel plate (Hamamatsu). For excitation of the samples at the Soret band, the frequency doubled pulses of a Ti:Sapphire laser (Coherent Mira 900, 400 nm, fwhm 200 fs) were used. The instrument response function was 65 ps, as measured at excitation wavelength using latex beads; the setup was previously described.[42] For data analysis the decay curves were deconvoluted and fitted using the least-squares method based on a Newton simplex algorithm.

Singlet Oxygen Generation. Photosensitizer-generated time-resolved singlet oxygen luminescence was measured at 1270 nm. A nanosecond Nd:YAG laser (BMI) equipped with an OPO (BMI) was used to excite the samples at 510 nm, and the luminescence signal was recorded by a germanium pin diode (Northcoast).[43] To calculate the singlet oxygen quantum yield, Φ_Δ, the solution of pheophorbide *a* in DMF was used as reference ($\Phi_\Delta = 0.52$[43]).

Photostability. Photostability measurements were performed using a diode-pumped Yb^+:YAG laser system (ELS VersaDisk) and a polychromator equipped with a cooled CCD matrix as a detector system (Lot-Oriel, Instaspec IV). The laser output was adjusted to 0.5 W at 515 nm (Gaussian distribution, diameter: 2.0 ± 0.2 mm). In an L-shaped setup, the steady-state fluorescence was detected perpendicular to the direction of excitation. About 2 mL of each sample was placed in cells with 10-mm optical path length and were permanently illuminated by cw-laser light. The optical density was 0.017 at excitation wavelength for all the samples. For 1.5 h, a steady-state fluorescence spectrum was recorded every minute using a basic automatization routine. The absorption spectra were taken before and after illumination to control the photodestruction of the samples.

Picosecond Transient Absorption Spectroscopy. To measure transient absorption spectra, a white light continuum was generated as a test beam in a cell with D_2O/H_2O mixture using intense 20-ps single pulses from a Nd:YLF laser (BMI) at 1047 nm. Before passing through the sample, the continuum radiation was split to get a reference spectrum. The transmitted as well as the reference beams were focused into two optical fibers and were recorded simultaneously at different traces on a CCD matrix (Lot-Oriel, Instaspec IV). The intense second harmonic of the same laser (524 nm) was used as a pump beam. The mechanical delay line allowed measuring the light-induced changes in the absorption spectrum at different time delays up to 15 ns after excitation. Details about the picosecond transient absorption setup were published.[44,45] The OD of all samples was 1.0 at the maximum of the Q-band absorption in cells with 5-mm optical path length.

Results

The synthesis of **6** (see Scheme 3) started with the preparation of the new fullerene hexaadduct **2**, which was obtained from the reaction of $\mathbf{C_{60}}$ with CBr_4 as bromine-transfer agent and DBU as base. The yield of the octahedral hexaadduct **2** was 42%, which was only possible due to the presence of DMA. DMA activates $\mathbf{C_{60}}$ and serves also as a regioselectivity-inducing agent.[46] The successful formation of **2** can be most easily seen in its ^{13}C NMR spectrum, which shows the typical three lines for a $\mathbf{C_{60}}$ hexaadduct with octahedral symmetry at 145.7, 141.1, and 69.1 ppm. Only one signal is found for the tertiary carbon atom of the BOC moiety at 78.9 ppm. Other spectroscopical data are also in accord with the structure of **2**. Pyropheophorbide *a* (**5**) was converted into an active ester; for reasons of stability and storage the *N*-hydroxysuccinimid ester **4** was chosen as best reagent for the next reaction step.

The BOC groups of the hexaadduct **2** were removed with methanolic HCl, to give after neutralization with triethylamine the dodecaamino-fullerene derivative **3**. This compound was rather unstable and was used directly without further characterization in a subsequent amide-formation reaction with the active ester **4**. With a 1.5-fold excess of **4** per amino group, the desired fullerene hexaadduct **6**, which carries 12 pyropheophorbide moieties, was obtained in excellent 74% yield (based on **2**). Not surprisingly, all resonances in the ^1H NMR spectrum of **6** appear as broad bands, which already indicate the interaction of the chromophores, most likely in the form of π-stacking. Interestingly, all pyropheorbide-related resonances of **6** are shifted to high field when compared to those of **4** with an average shift of about -0.4 ppm. Using a ring current model for porphyrins,[47] we can estimate an average distance of the pyropheophorbide units from each other of roughly 4−6 Å, which is in good accord with the value deduced from the molecular modeling studies (see below). Temperature-dependent NMR spectroscopy was done with **6** in $C_2D_2Cl_4$ at 0, 25, 50, and 70 °C with a concentration of $\sim 4 \times 10^{-3}$ M ($\sim 5 \times 10^{-2}$ M per dye) to see exchange broadening of the lines. No significant changes were visible in the spectra, which was also true for lower concentrations ($\sim 2 \times 10^{-3}$ M and 0.4×10^{-3} M). Obviously, the sidearms in **6** are flexible, and the exchange rates are of intermediate order on the NMR time scale. The concentration of the NMR sample of the monomeric compound **4** was $\sim 5 \times 10^{-2}$ M, which is with regard to the dye content the same as that for **6**. Because in this case sharp signals were found, we draw the conclusion that the broadening effects in the spectrum of **6** are attributed to internal processes and not to intermolecular interactions. The ^{13}C NMR spectrum of **6** is dominated by the resonances of the pyroPheo units. The electronic absorption spectrum of **6** shows the expected shape but has some interesting features (see Figure 1). A MALDI-TOF mass spectrum of **6** gives the molecular ion peak at 8724.3 (calculated 8722.6) which unambiguously proves the successful 12-fold amide formation.

The C_{60}-[6:0] hexaadducts **6**−**8** show good solubility in chlorinated hydrocarbons such as $CHCl_3$, CH_2Cl_2, and $C_2H_2Cl_4$. Moderate solubility is observed in THF and DMF, whereas toluene, acetonitrile, acetone, and alcohols fail to dissolve these compounds.

The steady-state absorption spectra of **6** and of the reference compounds **8** and **7** dissolved in DMF are presented in Figure 1a. The shape and spectral position of the absorption bands of **6** are practically the same as those of the reference **7**. The maximum of the Q_y-band absorption of **6** compared to that of

(41) Korth, O.; Hanke, T.; Rückmann, I.; Röder, B. *Exp. Tech. Phys.* **1995**, *41*, 25−36.
(42) Korth, O.; Hanke, T.; Röder, B. *Thin Solid Films* **1998**, *320*, 305−315.
(43) Spiller, W.; Kliesch, H.; Wöhrle, D.; Hackbarth, S.; Röder, B.; Schnurpfeil, G. *J. Porphyrins Phthalocyanines* **1998**, *2*, 145−158.
(44) Rückmann, I.; Zeug, A.; Herter, R.; Röder B. *Photochem. Photobiol.* **1997**, *66*, 576−584.
(45) Zimmermann, J.; Zeug, A.; Röder, B. *Phys. Chem. Chem. Phys.* **2003**, *5*, 2964−2969.
(46) Lamparth, I.; Maichle-Mössmer, C.; Hirsch, A. *Angew. Chem., Int. Ed. Engl.* **1995**, *34*, 1607.
(47) Abraham, R. J.; Bredford, G. R.; McNeillie, D.; Wright, B. *Org. Magn. Reson.* **1980**, *14*, 418−425.

Scheme 3. Synthesis of C_{60} [6:0]-Hexaadduct Carrying 12 Pyropheophorbide *a* Molecules; See Text for Details

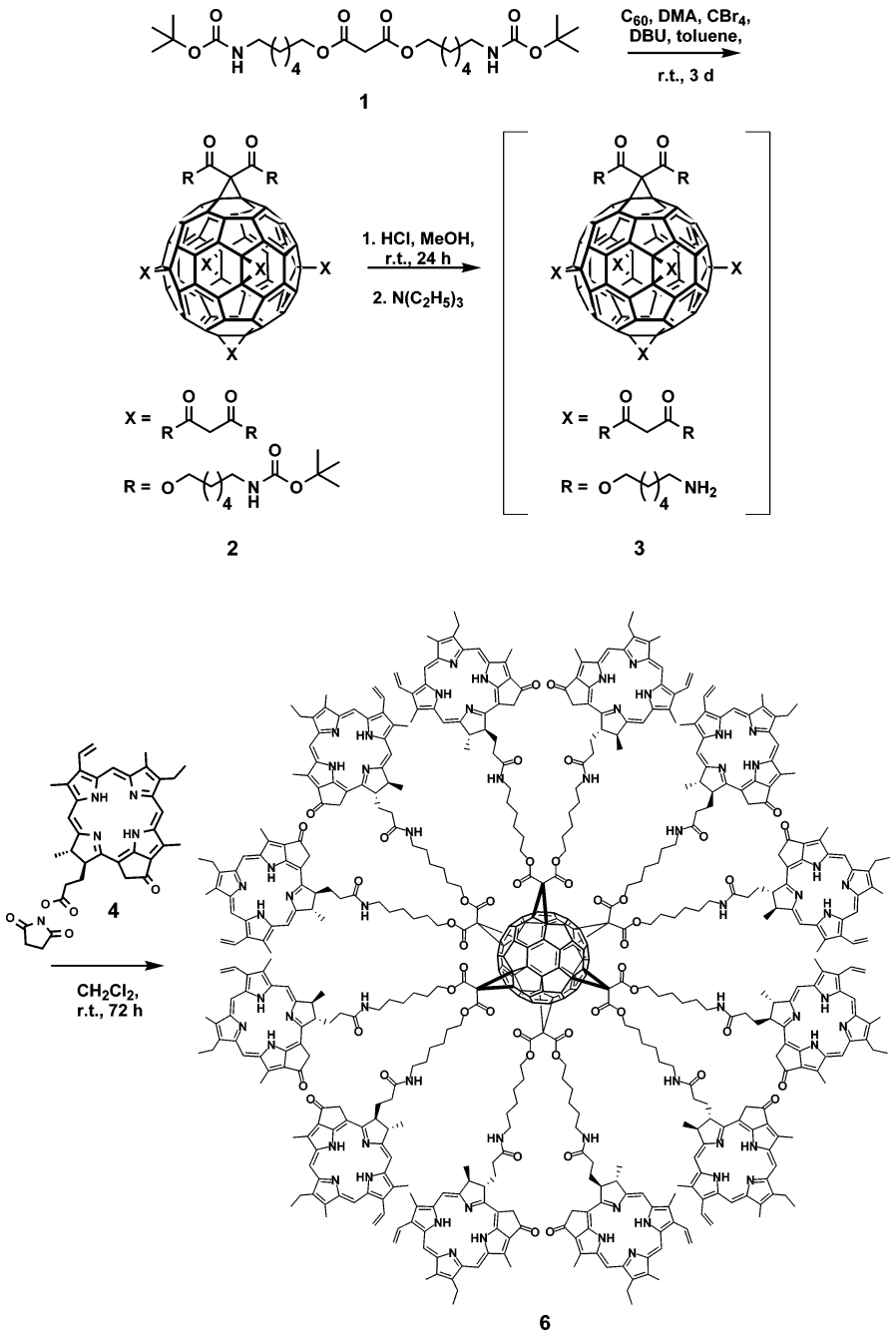

8 is shifted bathochromically by 1.5 nm, while the Soret band of **6** is split and the second peak with lower absorbance has its maximum at 403 nm (see also Table 1). The extinction coefficients of the Soret band were determined to have values of 8.8×10^5, 4.1×10^5, and 1.6×10^5 M^{-1} cm^{-1} for **6**, **7**, and **8**, respectively, at 414 nm in DMF. Obviously, **7** does not reach the expected roughly 3-fold increase, nor does **6** attain the 6-fold level of the extinction coefficient of the reference system **8**.

These effects already indicate the interactions between dye molecules coupled to one fullerene; however, the results of such interactions are more visible in fluorescence. It should be emphasized that photoinduced changes in the steady-state fluorescence become more pronounced for **6** than for **7**. The maxima of the emission spectra of **6** and **7** are red-shifted by 4.5 and 2.5 nm, respectively, compared with that of **8** (Figure 1b and Table 1). Moreover, the shape of the fluorescence spectrum of **6** is changed: it becomes broader and the gap between main band and vibronic shoulder is not as pronounced as it is for the **8** compound. The estimations have shown that the fluorescence quantum yield of **6** is about 3 and 10 times smaller compared to that of **7** and **8**, respectively.

On the basis of our previous results[33] and steady-state fluorescence measurements, we expected to detect the fluorescence decay of the three studied compounds at two different wavelengths. The first of them, 675 nm, corresponds to the maximum of the fluorescence spectrum of **8**. The second one at 707 nm has been selected because the difference between the fluorescence spectra of **8** and both **7** and **6** is highly

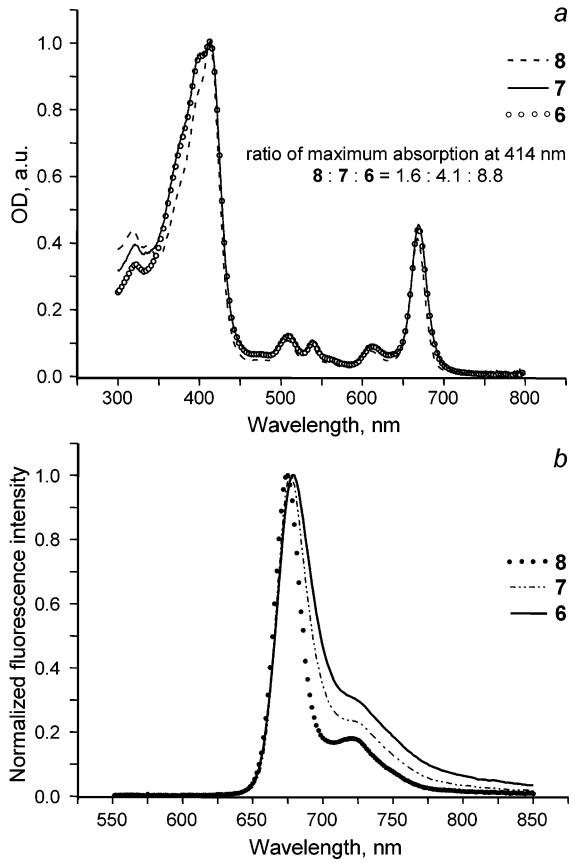

Figure 1. Steady-state absorption (a) and fluorescence (b) spectra of **8**, **7**, and **6** in DMF, $\lambda_{exc} = 414$ nm.

pronounced. For **8**, a single-exponential decay of the first excited singlet state with a lifetime $\tau = 5.7$ ns (see Figure 2 and Table 1) at both registration wavelengths was obtained. **6** and **7** have a more complex fluorescence decay. For **7**, a three exponential fit results in the following decay times: $\tau_1 = 5.7$ ns, $\tau_2 = 3.7$ ns, and $\tau_3 = 1.0$ ns.[33] The second component gives the dominant contribution to the fluorescence signal at both registration wavelengths, whereas the third decay time has its maximum amplitude at 707 nm. The fluorescence of **6** decays much faster than that of **7**. Moreover, the first decay time of **7** (5.7 ns) has the same value as the fluorescence lifetime of **8**, but for **6** this decay time was not resolved anymore (Table 1). The longest decay component has a value of 4.9 ns at the registration wavelength of 675 nm and 3.6 ns at 707 nm. The contribution of it to the overall fluorescence decay of **6** is minimal at both registration wavelengths.

Using picosecond transient absorption spectroscopy (ps-TAS), we observed an additional decay time for recovery of the ground-state population of **8**. A double exponential fit led to two decay times: 700 ps and 5.7 ns; the amplitude of the short component was three times smaller than that for the long one. Moreover, it should be remembered that this short decay time was not observed in the time-resolved fluorescence experiments. The recovery of the ground states of **7** and **6** is very fast (see Figure 3), and decay components with values of 71 and 23 ps, respectively, were resolved. For both samples the second decay time (1.1 and 0.27 ns, respectively) is in good agreement with the decay times obtained using TCSPC technique. Unfortunately, due to the low values of the ΔOD signal at longer delay times and the poor signal-to-noise ratio of measurements taken for **7** and **6**, the long decay times (3.7 and 5.7 ns for **7** and 4.9 or 3.6 ns and 1.5 ns for **6**; see Table 1) could not be fitted with adequate or sufficient accuracy.

Because of lower fluorescence and the faster ground-state population recovery of **6** compared to both **8** and **7**, it could be expected that the intersystem crossing (ISC) quantum yield as well as the singlet oxygen generation of **6** are also reduced (with respect to the values of the reference compounds). Using time-resolved methods (ps-TAS and detection of the singlet oxygen luminescence), we obtained an ISC quantum yield of $\Phi_{ISC} = 0.14$ and a quantum yield of singlet oxygen generation of $\Phi_{\Delta} = 0.13$ for **6** in DMF, whereas for **8** and **7** these values were estimated to be 0.49, 0.23 (Φ_{ISC}) and 0.43, 0.22 (Φ_{Δ}), respectively (Table 1).

During illumination with cw-laser radiation (see "Photostability" in Experimental Section), the fluorescence quantum yield of all three compounds is reduced (Figure 4a). For all of them, this reduction has monotonic character, and after 1.5 h the fluorescence quantum yields were 15, 33, and 38% less than their initial values for **6**, **7**, and **8**, respectively. The absorbance of the samples decreases monotonically with increasing illumination time. No changes of spectral position or shape of the absorption bands were observed. After 1.5 h of illumination the fluorescence spectrum of **7** became similar to that of **8** (Figure 4b). For **6**, the maximum of the fluorescence spectrum is hypsochromically shifted compared to its initial position, and moreover, the bandwidth becomes narrow. It should be also mentioned that no recovery in the dark has been found. It was proved to be taking absorption as well as fluorescence spectra in 1 day after illumination. The shape, spectral position, and intensity of the bands were the same as measured after 90 min of illumination.

Discussion

The strong reduction of the fluorescence as well as singlet oxygen quantum yield, red-shifted absorption and fluorescence spectra, and non-monoexponential fluorescence decay of **6** are an impeachable proof for intramolecular interactions between pyropheophorbide *a* chromophores. All results presented above are well-correlated with the model that was proposed in our previous article[33] where the photophysical properties of **7** were investigated. It was shown that stepwise intramolecular Förster energy transfer between pyropheophorbide *a* molecules coupled to one fullerene moiety causes a very fast and efficient delivery of the excitation to an energy trap formed by two stacked and excitonically interacting pyropheophorbide *a* chromophores. As a result, the fluorescence as well as the singlet oxygen quantum yield of **7** are reduced compared to those values of the reference **8**.[33]

For **6**, the interactions between the pyropheophorbide *a* chromophores covalently coupled to one fullerene should become stronger than those for **7** due to the higher local concentration of pyropheophorbide *a* moieties. Indeed, based on molecular modeling (HyperChem program, MM+ method at room temperature and in a vacuum[48]) it could be shown that the average distance between two neighboring pyropheophorbide

(48) *HyperChem*, version 7.5; HyperCube, Inc.: Gainesville, FL, 2004.

Table 1. Photophysical Parameters of **8**, **7**, and **6** in DMF

sample	Soret (nm)	Q^a (nm)	$\lambda_{max}{}^b$ (nm)	$\tau_{fl}{}^c$ (ns) 675 nm		$\tau_{fl}{}^c$ (ns) 707 nm		$\Phi_{fl}{}^d$	$\Phi_{\Delta}{}^e$	$\Phi_{ISC}{}^f$
8	414	668	674.5	{0.7}	(−)	{0.7}	(−)	1	0.43	0.49
				5.7	(1.0)	5.7	(1.0)			
7	414	670	677	{0.071}	(0.40)	{0.071}	(−)	0.33	0.22	0.24
	403			1.0	(0.11)	1.0	(0.29)			
				3.7	(0.39)	3.7	(0.62)			
				5.7	(0.1)	5.7	(0.09)			
6	414	669.5	679	{0.023}	(0.56)	{0.023}	(0.50)	0.098	0.13	0.14
	403			0.34	(0.19)	0.28	(0.20)			
				1.5	(0.20)	1.5	(0.23)			
				4.9	(0.05)	3.6	(0.07)			

[a] Peak maxima of the absorption Q-band. [b] Fluorescence maxima. [c] Fluorescence decay times at different registration wavelengths. For all compounds the first decay times are shown in fences ({ }) because their values could not be estimated correctly with direct time-resolved fluorescence measurements (due to insufficient time resolution). These times were obtained by ps-TAS experiments. In parentheses the relative amplitudes of the decay components are given. [d] Fluorescence quantum yields (relative to **8**). [e] Quantum yields of photosensitized singlet oxygen generation. [f] Intersystem crossing quantum yields.

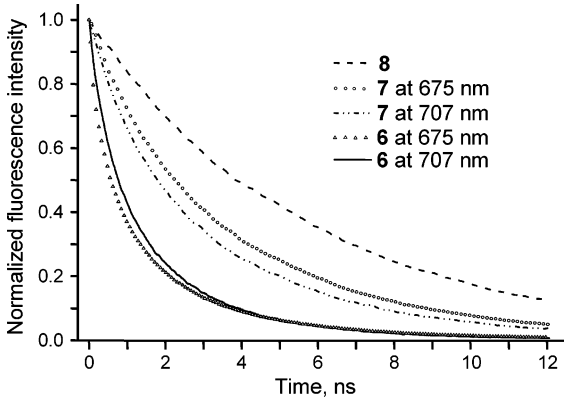

Figure 2. Fluorescence decay of **8**, **7**, and **6** in DMF at different registration wavelengths, $\lambda_{exc} = 400$ nm.

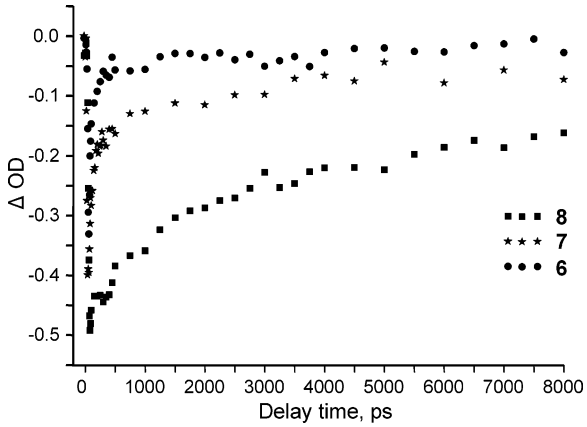

Figure 3. Transient absorption of **8**, **7**, and **6** in DMF at different delay times. Registration wavelength is 668 nm.

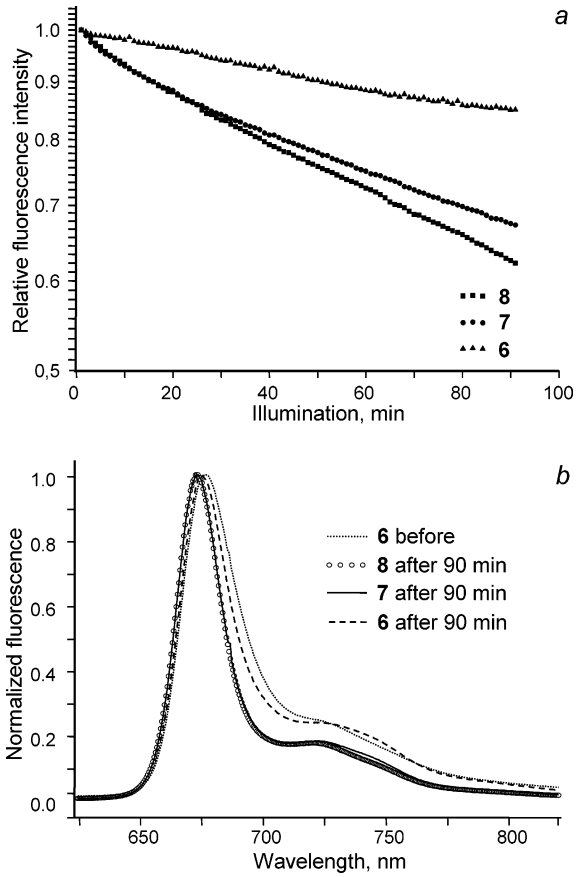

Figure 4. Fluorescence intensities during illumination (a) and fluorescence spectra after one and a half hour of illumination (b) of **8**, **7**, and **6** in DMF.

a units belonging to one fullerene moiety ($\bar{R}$) is shorter for **6** than for compound **7**. In Figure 5, for both **7** and **6** as examples, energetically optimized conformations are shown. Although each of these pictures shows just one possible conformation, they visualize an effect that was visible for all calculations for **7** and **6**. The pyropheophorbide *a* molecules covalently linked to the fullerene moiety have a strong tendency to stack with each other. Moreover, for **6** this stacking has a higher probability than for **7**. The value of $\bar{R}$ was estimated to be 6 and 14 Å for **6** and **7**, respectively. It should be mentioned that since the calculations have been carried out in a vacuum, in solution the stacking effects should be reduced, otherwise, the reduction of the fluorescence as well as the singlet oxygen quantum yields for **7** had to be much stronger than observed experimentally.

Due to the fact that the calculated Förster radius for dipole−dipole energy transfer between pyropheophorbide *a* chromophores (52 Å) is much longer than the average distance between neighboring dye molecules attached to one fullerene moiety,

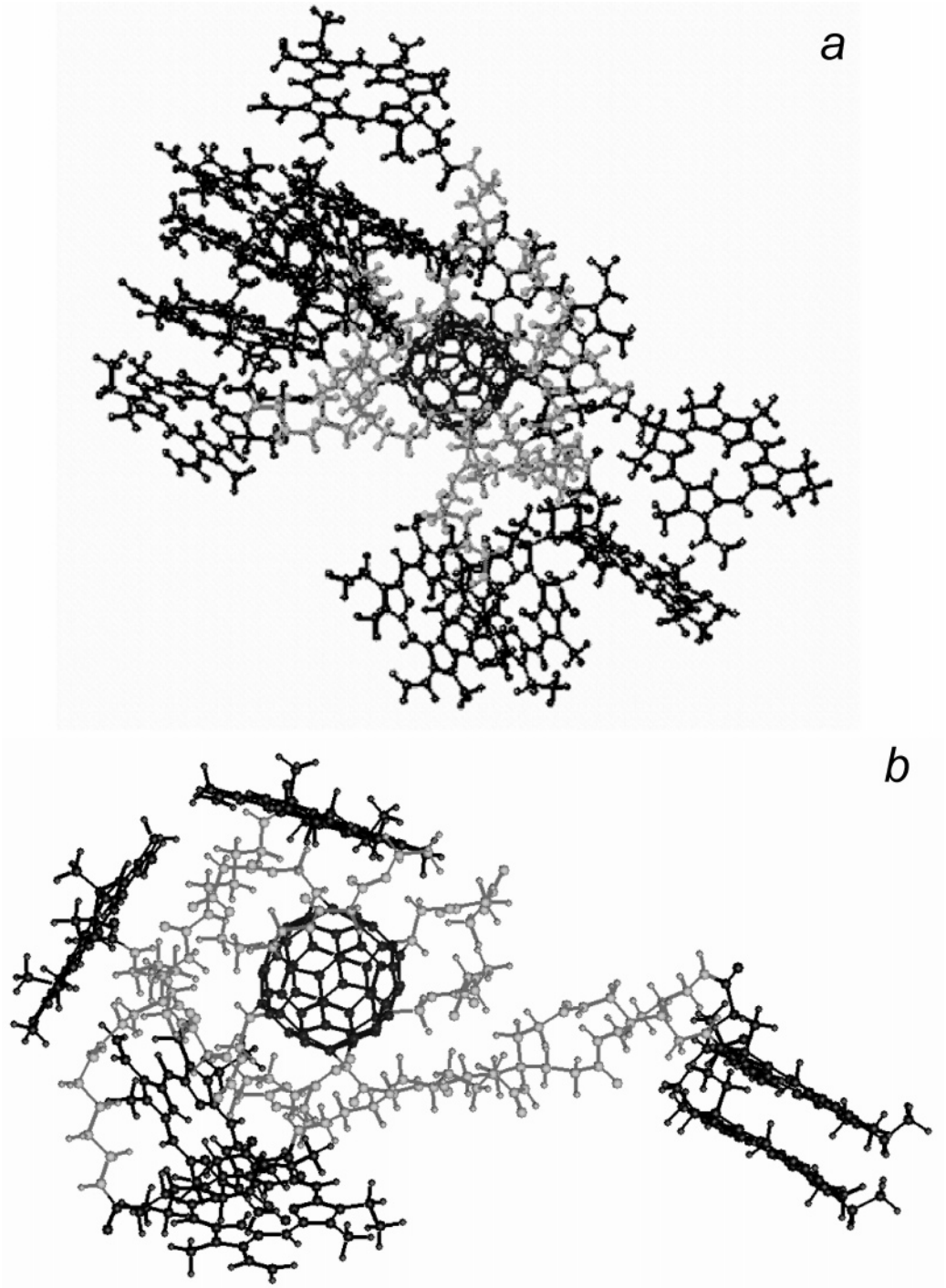

Figure 5. Possible conformations of **6** (a) and **7** (b) at room temperature; pyropheophorbide *a* moieties are shown in black.

the stacking of just one pair of chromophores leading to excitonic interaction (and as result to the formation of an energy trap) is sufficient for a very efficient quenching of the fluorescence of the whole complex. Because of the higher trap formation probability for **6** than for **7** (due to abovementioned higher local concentration of pyropheophorbide *a* chromophores), it is understandable that the fluorescence of **6** is weaker than that of **7**. Moreover, the delivery of the excitation to the traps should occur faster.

It is known from literature[49−53] that in special cases the formation of chlorophyll and porphyrin dimers has changed the absorption and fluorescence spectra as well as reduced fluorescence quantum yields compared to those of monomeric molecules. The same effects were observed for both **7** and **6** (see Figure 1a).

It should be remembered that two different types of energy traps were proposed to exist in the **7** molecular system.[33] One of them (**Trap I**) is formed via face-to-face stacking of two

(49) Osuka, A.; Wada, Y.; Shinoda, S. *Tetrahedron* **1996**, *52*, 4311−4326.
(50) Hoff, A. J.; Amesz, J. P. In *Chlorophylls*; Scheer, H., Ed.; CRC Press: Boca Raton, FL, 1991; pp 723−738.
(51) Osuka, A.; Maruyama, K. *J. Am. Chem. Soc.* **1988**, *110*, 4454−4456.
(52) (a) Bucks, R. R.; Boxer, S. G. *J. Am. Chem. Soc.* **1982**, *104*, 340−343. (b) Boxer, S. G.; Bucks, R. R. *J. Am. Chem. Soc.* **1979**, *101*, 1883−1885. (c) Boxer, S. G.; Closs, G. L. *J. Am. Chem. Soc.* **1976**, *98*, 5406−5408.
(53) Kosaka N.; Tamiaki, H. *Eur. J. Org. Chem.* **2004**, 2325−2330.

pyropheophorbide *a* molecules. The shortest component of the fluorescence decay of **7** (1.0 ns) observed in time-resolved measurements was associated with the emission of this **Trap I**. The second type of energy trap (**Trap II**) has the oblique geometry of the interacting pyropheophorbide *a* molecules. Due to the strength of excitonic interactions between pyropheophorbide *a* chromophores in **Trap II**, which is weaker than that in **Trap I**, the fluorescence quantum yield of **Traps II** should be higher than that of **Trap I** and the lifetime of the excited state should be longer. But both types of energy traps have lower fluorescence quantum yields and bathochromically shifted emission compared to the monomeric pyropheophorbide *a*. These conclusions are in a good agreement with results obtained for several dimers of reduced porphyrins (and among them pyropheophorbide *a* dimers).[49,51−55]

Applying the model described above and according to the data obtained in the time-resolved fluorescence measurements, it was assumed that **Traps I** in **6** have a fluorescence lifetime of about 300 ps, whereas **Traps II** could be associated with the fluorescence decay time of about 1.5 ns (see Table 1). These decay components have practically the same amplitude at both registration wavelengths. Moreover, it seems that the longest decay time of **6** (4.9 ns at 675 nm and 3.6 ns at 707 nm) is a result of the superposition of the fluorescence decay time of monomeric pyropheophorbide *a* chromophores and that of **Traps II**. Such a conclusion is supported by the fact that the value of this decay time is strongly reduced when the fluorescence decay was detected at 707 nm, where the contribution of the traps to the fluorescence is high compared to the registration at 675 nm, where emission of the monomeric dye molecules has its maximum. It should be mentioned here that due to the spectral positions of the fluorescence band of pyropheophorbide *a* (**5**) and the absorption band of hexasubstituted $\mathbf{C_{60}}$ an energy transfer from photoexcited **5** to the fullerene core is energetically unfavorable. This contrasts previously found results for hexasubstituted anthracene−fullerene conjugates.[56]

Due to the higher probability of the trap formation in **6** compared to **7** it is not surprising that the steady-state emission of **6** is more red-shifted than that of **7** with respect to the **8** fluorescence spectrum. Furthermore, the broadening of the red edge of the fluorescence spectrum of **6** shows the high contribution of the trap emission to the fluorescence signal.

In the presence of one or more traps in a complex an additional decay time arises, which represents the probability of energy transfer to the trap. Using ps-TAS technique, we estimated this time to be 71 ps for **7** and 23 ps for **6**. It can be seen that the faster delivery of the excitation energy to the trap in **6** is due to shorter distances between the pyropheophorbide *a* chromophores and a higher probability of trap formation compared with the same parameters of **7**.

The additional decay time for **8** (which was not resolved in TCSPC measurements) can be explained if we take into account the fact that the fluorescence quantum yield of a dimer formed by two interacting pyropheophorbide *a* molecules has a lower value compared to that of the monomeric molecule. Due to the length and high flexibility of the carbon chains, the pyropheophorbide *a* chromophores are able to form such dimers also in **8**. The population of the first excited state of these dimers occurs only via direct absorption of the excitation light but not via energy transfer from monomeric dye moieties because of the low concentrations used in all experiments. In time-resolved fluorescence measurements, the fluorescence intensity of the dimers is practically negligible compared to the strong emission of the monomeric pyropheophorbide *a* due to the above mentioned facts. On the contrary, in ps-TAS experiments a bleaching of the ground-state absorption is detected. But the dimers usually have only a slightly reduced absorption cross section compared to that of a monomeric dye, and as result, the recovery of their ground-state population can be easily resolved in TAS. Moreover, the dimer formation could explain the 30% reduction of the fluorescence quantum yield of **8** compared to that of a pyroPheo-8-hydroxyoctylester compound.[31]

The singlet oxygen quantum yield of **6** is only three times less than that of **8**, which means that the traps must be able to undergo an intersystem crossing to allow further energy transfer to molecular oxygen. The probability of this process should be higher than the probability of the trap to emit light since the fluorescence quantum yield of **6** is 10 times lower than the one of **8**. This fact correlates well with proposals of Kasha's theory of excitonic interactions.[57−59]

The photostability of molecular systems strongly depends on their ISC as well as their singlet oxygen generation quantum yields. During the light illumination, the excitation is efficiently delivered to the traps existing in both **7** and **6**. Because the traps have a lower ISC and singlet oxygen quantum yields compared to monomeric pyropheophorbide *a*, the photostability of **7** and **6** is higher than that of **8** (Figure 4a). As compared to **7**, the interactions between pyropheophorbide *a* molecules in **6** are stronger, leading to a higher number of formed traps. Therefore, this compound exhibits a much higher photostability than the reference compounds. Due to high probability of energy transfer between pyropheophorbide *a* molecules in both **7** and **6**, the excitation energy is very quickly delivered to the traps which undergo the photodestruction in the first place. The hypsochromic shift of the fluorescence maximum and reduction of intensity at the red edge of the fluorescence spectra, where the trap emission gives the major contribution in the fluorescence signal (see Figure 4b), are proof of the above-discussed model.

Conclusion

The new compound **6** which carries 12 pyropheophorbide molecules attached to $\mathbf{C_{60}}$ was prepared, and its photophysical properties were intensively studied. It was shown that in both **7** and **6** the pyropheophorbide *a* molecules covalently linked to the fullerene undergo very efficient energy transduction as well as partly excitonic interactions within the system. The latter process already occurs in **8**, which contains only two chromophores. For **6**, the strength of interactions between pyropheophorbide *a* units is higher than those for **7** due to a higher local

(54) Zenkevich, E. I.; Knyukshto, V. N.; Shulga, A. M.; Kuzmitsky, V. A.; Gael, V. I.; Levinson, E. G.; Mironov, A. F. *J. Lumin.* **1997**, *75*, 229−244.
(55) Kozyrev, A. N.; Suresh, V.; Das, S.; Senge, M. O.; Shibata, M.; Dougherty, T. J.; Pandey, R. K. *Tetrahedron* **2000**, *56*, 3353−3364.
(56) (a) Diekers, M.; Luo, C.; Guldi, D. M.; Hirsch, A. *Chem.−Eur. J.* **2002**, *8*, 979−991. (b) Diekers, M.; Hirsch, A.; Luo, C.; Guldi, D. M.; Bauer, K.; Nickel, U. *Org. Lett.* **2000**, *2*, 2741−2744.
(57) McRae, E. G.; Kasha, M. *J. Chem. Phys.* **1958**, *28*, 721−722.
(58) McRae, E. G.; Kasha, M. In *Physical Processes in Radiation Biology*; Academic Press: New York, 1964; p 23.
(59) Kasha, M.; Rawls, H. R.; Ashraf El-Bayoumi, M. *Pure Appl. Chem.* **1965**, *11*, 371−392.

concentration of dye molecules, which results in shorter distances between them. As a consequence, the excitation energy is delivered rapidly (within 23 ps) to traps formed by stacked pyropheophorbide *a* chromophores resulting in the reduction of the fluorescence, the intersystem crossing, and the singlet oxygen quantum yields compared to the values of the reference compounds. Nevertheless, **6** is more photostable than both **8** and **7**. This motif will be further expanded.

Acknowledgment. We thank the DFG (E.A.E., B.R.: Grant No. RO 1042/9-3; E.A.E., B.R., M.M.: Grant No. RO 1042/11-1; A.H., M.H., N.J.: Grant No. HI 468/11-1). We also thank Mrs. Gisela Wöhlecke (Berlin) for technical assistance and Priv.-Doz. Dr. Andreas Humeny (Erlangen) for performing the MALDI-TOF experiments.

JA0503581